HHS Public Access

Author manuscript

Endocr Relat Cancer. Author manuscript; available in PMC 2018 August 08.

Published in final edited form as:

Endocr Relat Cancer. 2011 October ; 18(5): 613–626. doi:10.1530/ERC-10-0289.

Inhibition of gap junction transfer sensitizes thyroid cancer cells to anoikis

Kirk Jensen,
Department of Pediatrics, Uniformed Services University of the Health Sciences, 4301 Jones Bridge Road, Bethesda, Maryland 20814-4712, USA

Aneeta Patel,
Department of Pediatrics, Uniformed Services University of the Health Sciences, 4301 Jones Bridge Road, Bethesda, Maryland 20814-4712, USA

Joanna Klubo-Gwiezdzinska[1], **Andrew Bauer**, and
Department of Pediatrics, Uniformed Services University of the Health Sciences, 4301 Jones Bridge Road, Bethesda, Maryland 20814-4712, USA

Vasyl Vasko
Department of Pediatrics, Uniformed Services University of the Health Sciences, 4301 Jones Bridge Road, Bethesda, Maryland 20814-4712, USA

[1]Division of Endocrinology, Department of Medicine, Washington Hospital Center, Washington, District of Columbia 20010–2975, USA

Abstract

Resistance to anoikis (matrix deprivation-induced apoptosis) is a critical component of the metastatic cascade. Molecular mechanisms underlying resistance to anoikis have not been reported in thyroid cancer cells. For an *in vitro* model of anoikis, we cultured follicular, papillary, and anaplastic thyroid cancer cell lines on poly-HEMA-treated low-adherent plates. We also performed immunohistochemical analysis of human cancer cells that had infiltrated blood and/or lymphatic vessels. Matrix deprivation was associated with establishment of contacts between floating thyroid cancer cells and formation of multi-cellular spheroids. This process was associated with activation of gap junctional transfer. Increased expression of the gap junction molecule Connexin43 was found in papillary and anaplastic cancer cells forming spheroids. All non-adherent cancer cells showed a lower proliferation rate compared with adherent cells but were more resistant to serum deprivation. AKT was constitutively activated in cancer cells forming spheroids. Inhibition of gap junctional transfer through Connexin43 silencing, or by treatment with the gap junction disruptor carbenoxolone, resulted in loss of pAKT and induction of apoptosis in a cell-type-specific manner. In human thyroid tissue, cancer cells that had infiltrated blood vessels showed morphological similarity to cancer cells forming spheroids *in vitro*. Intra-vascular cancer

Correspondence should be addressed to V Vasko; vvasko@usuhs.mil.

Supplementary data
This is linked to the online version of the paper at http://dx.doi.org/10.1530/ERC-10-0289.

Declaration of interest
The authors declare that there is no conflict of interest that could be perceived as prejudicing the impartiality of the research reported.

cells demonstrated prominent AKT activation in papillary and follicular cancers. Increased Connexin43 immunoreactivity was observed only in intra-vascular papillary cancer cells. Our data demonstrate that establishment of inter-cellular communication contributes to thyroid cancer cell resistance to anoikis. These findings suggest that disruption of gap junctional transfer could represent a potential therapeutic strategy for prevention of metastases.

Introduction

Metastasis comprises a multitude of events, including tumor cell invasion of the surrounding tissue and intravasation into the lymphatic or systemic vasculature, survival in a non-adherent environment, extravasation from vessels, and ‘seeding’ at a distant site. Numerous observations support the notion that epithelial to mesenchymal transition (EMT) plays a central role in cancer cell invasion (Thiery 2002). During progression to metastatic competence, carcinoma cells change their adhesive properties, activate proteolysis, and become motile, allowing them to leave the primary tumor.

With dissemination away from the tissue origin into the lymphatic or vascular compartment, tumor cells are confronted by an environment deprived of normal physiological adhesion signals. Epithelial cells have very low survival rates in the circulation, and loss of contact with the extra-cellular matrix causes epithelial cells to undergo programmed cell death, termed anoikis (Wang 2004). Matrix-independent survival of metastatic cancer cells during passage through the lymph and/or blood compartment is a critical component of the metastatic cascade. It has been shown that in malignant lesions, cancer cell sub-populations selected for increased metastatic potential demonstrate an increased resistance to anoikis compared with the parental cells (Liotta & Kohn 2004).

The survival of carcinoma cells in a suspension culture system is considered to be a model of anoikis resistance. Gene expression profiling of anoikis-resistant cancer cells shows over-expression of genes coding for cell adhesion molecules but down-regulation of molecules controlling cell cycle progression (Zhang *et al.* 2008). In addition, cells growing in suspension show activation of oncogenic receptor tyrosine kinases and their downstream signaling pathways, contributing to anchorage-independent survival. The critical role of phosphatidylinositol 3-kinase (PI3K)/AKT signaling in anchorage-independent survival and growth has been demonstrated in multiple cancer cell lines. It has been shown that cells transfected with constitutively active forms of either PI3K or AKT do not undergo anoikis, whereas inhibition of PI3K induces anoikis (Khwaja *et al.* 1997). Transcriptional repression of phosphate and tensin homolog (PTEN) located on chromosome 10 results in constitutive AKT activation and may also play a role in the development of anoikis resistance (Chappell *et al.* 2005).

Thyroid cancer is a common endocrine malignancy and many thyroid cancer patients present with metastases at the time of surgery. We previously demonstrated that thyroid cancer cells in the invasive front of human tumors undergo EMT and that metastatic thyroid cancers are characterized by over-expression of mesenchymal markers such as osteopontin and vimentin (Vasko *et al.* 2007). In addition, activation of the PI3K/AKT pathway plays an important role in thyroid cancer progression (Hou *et al.* 2007), and nuclear activation of AKT has been

described in thyroid cancer cells invading into adjacent tissues (Vasko *et al*. 2004). Much less is known about the mechanisms that allow thyroid cancer cell survival as they detach from the primary tumor and invade into blood vessels.

In this study, we sought to characterize the behavior of thyroid cancer cells that lose their attachment to an extra-cellular matrix. In an effort to define the molecular mechanisms involved in resistance of thyroid cancer cells to anoikis, we compared anti-apoptotic signaling pathways in thyroid cancer cell lines growing in adherent and low-adherent conditions. Finally, to confirm our *in vitro* findings, we examined human thyroid tissue samples using immunohistochemical analysis of cancer cells that had invaded into blood or lymphatic vessels.

Materials and methods

Human thyroid tissue and cell culture

The protocol was approved by the Human Use Committee at the Uniformed Services University of the Health Sciences and conformed to the standards of human research from the Helsinki Mandate. Paraffin-embedded thyroid tissue samples were obtained from 35 papillary thyroid cancers (PTCs) and ten follicular thyroid cancers (FTCs).

Human thyroid cancer cell lines derived from FTC (FTC133 and WRO-82), follicular cancer metastases (FTC236 and FTC238), PTC (TPC1, BCPAP, and KTC1), and anaplastic cancer (SW1736) were obtained from Dr Motoyasu Saji (The Ohio State University) with permission from the researchers who originally established the cell lines. All cell lines had been tested and authenticated by DNA analysis to be of thyroid origin (Schweppe *et al*. 2008). In our laboratory, we examined expression of PAX8 and TTF1 to confirm thyroid origin of these cell lines. These cell lines express common thyroid oncogenes including *BRAF V600E* (BCPAP, KTC1, and SW1736) or *RET/PTC1* (TPC1; Schweppe *et al*. 2008) or have loss of PTEN expression (FTC133; Weng *et al*. 2001). In our laboratory, we examined expression of PTEN by western blot and, consistent with previous reports, PTEN protein was not detected in FTC133 cells as well as in FTC236 and FTC238 cell lines that derived from the metastatic lesions of the same patient.

Cancer cells were propagated in RPMI 1640 medium (Invitrogen) supplemented with 5% of fetal bovine serum. Cells were maintained in either adherent cell culture plates or low-adherent cell culture conditions (poly-HEMA-treated plates). A pharmacological inhibitor of PI3K/AKT signaling (LY-294002), an inducer of cell cycle arrest (docetaxel), a gap junction disruptor (carbenoxolone), a glucocorticoid (dexamethasone), and a mineralocorticoid (aldosterone) were obtained from Sigma Chemical Co. LY303511 (the structural analog of LY-294002 which does not inhibit PI3K) was obtained from Santa Cruz Biotechnology (Santa Cruz, CA, USA).

siRNA transfections

FTC133, TPC1, BCPAP, and SW1736 cells were transfected with Connexin43-specific siRNAs (Invitrogen #1320003) or with Stealth RNAi siRNA-negative control. To avoid non-specific effects, experiments were performed with three different types of Connexin43

siRNAs. RNAi duplex–Lipofectamine complexes were prepared using RNAiMAX transfection reagent (Invitrogen). The efficiency of silencing was assessed by detection of Connexin43 mRNA using quantitative real-time PCR and western blot. Assays were performed 48 h after the beginning of the transfections.

Cell proliferation and cell viability assays

Cell proliferation rate was determined by cell counting using Vi-CELL Cell Viability Analyzer from Beckman Coulter (Fullerton, CA, USA). Cell viability was determined by evaluation of mitochondrial membrane potential with a fluorogenic lipophilic cation (JC-1; Cayman Chemical Company, Ann Arbor, MI, USA). In cells with high mitochondrial potential, JC-1 spontaneously forms complexes (J aggregates) with intense red fluorescence at 570–610 nm. In cells with low mitochondrial potential, JC-1 remains in a monomeric form that fluoresces green at 535 nm. Detection of mitochondrial membrane potential was performed according to the manufacturer's instructions followed by fluorescent microscopy. The ratio between intensity of red and green fluorescent signals was calculated to determine the relative cell viability. Dead cells were also detected using propidium iodine staining. All experiments were repeated at least three times, and the average values ± S.D. of representative experiments are reported.

Cell dye transfer assay

Gap junction function was evaluated as described by Goldberg *et al.* (1995). Gap junction intercellular communication was followed by labeling cells with calcein–acetoxymethyl ester (calcein AM). Once inside the cell, calcein AM is cleaved by non-specific esterases into calcein, which can no longer diffuse across the cell membrane, but with a molecular weight of 994 Da can be transferred through gap junctions from donor cells to recipient cells. Donor cells were labeled with 1 μM calcein AM (Invitrogen) for 20 min at room temperature and visualized by fluorescent microscopy. Donor cells were also labeled with 2 μM CM-DiI, a red fluorescent dye that does not transfer between cells. Labeled donor and unlabeled recipient cells were then trypsinized and seeded onto adherent or low-adherent plates at a 1:10 donor/recipient ratio and examined by fluorescent microscopy at 6, 12, and 24 h. For each experimental condition, the average number of calcein-containing cells was determined by microscopy and normalized to that of control cultures. Flow cytometry was performed using BD LSRII cell analytic flow cytometer to calculate the average number of cells that received calcein from donor cells.

RNA extraction and quantitative RT-PCR

Total RNA was isolated from thyroid cancer cells using RNeasy Mini Kit (Qiagen) according to the manufacturer's protocol. SYBR green-based qPCR master mixes were obtained from SuperArray Bioscience Corporation (Frederick, MD, USA).

Quantitative RT-PCR screening of genes with an established role in cancer was performed using the Cancer Drug Resistance & Metabolism PCR Array (PAHS-004) and Angiogenesis PCR Array (PAHS-024) from SuperArray Bioscience Corporation.

Protein extraction and western blot analysis

Thyroid cancer cells were incubated with ice-cold cell lysis buffer, scraped, centrifuged, and the supernatant was stored at −80 °C. Twenty-five micrograms of total protein lysate were suspended in reduced SDS sample buffer and the lysates were subjected to SDS–PAGE (4–12%). The separated proteins were transferred to a nitrocellulose membrane (Invitrogen) by electrophoretic blotting.

Membranes were incubated overnight with the primary antibody against vimentin and β-actin (Sigma–Aldrich, Inc.), p-AKT1/2/3 (Ser473), total AKT, and cleaved caspase 3 (Cell Signaling Technology Danvers, MA, USA); *N*-Cadherin, *E*-Cadherin, Connexin43, Connexin31, integrins α6, and β4; cyclin D1 (Santa Cruz Biotechnology); and p27 (BD Biosciences Pharmingen, San Diego, CA, USA).

Immunodetection of proteins was performed using the Li-Cor Odyssey imaging system (LI-COR Biosciences, Lincoln, NE, USA). After normalization to the level of β-actin, quantification of Connexin43 protein was performed.

Immunostaining

Immunostaining was performed on paraffin-embedded tissue sections. Endogenous peroxidase activity was quenched by incubation in 3% hydrogen peroxide. Sections were incubated overnight with primary antibodies and immunostaining was performed using the Vector Universal Kit (Vector Laboratories, Burlingame, CA, USA) according to the manufacturer's instruction.

For immunostaining of cancer cell lines, adherent thyroid cancer cells were cultured overnight on eight-chambered SuperCell Culture Slides (Fisher Scientific, Pittsburgh, PA, USA) and then fixed in formalin for 15 min. Non-adherent cells were transferred from suspension to slides using a standard cytospin protocol and then fixed in formalin for 15 min. After washing, cells were incubated overnight at 4 °C with anti-pAKT1/2/3 (Ser473) or anti-p27 antibody. Slides were then incubated at room temperature for 1 h with species-specific Alexa 488-conjugated secondary antibody.

Results

Thyroid cancer cells form multi-cellular spheroids in low-adherent condition

In adherent conditions, all examined thyroid cancer cell lines at 50% of confluency demonstrated spindle, mesenchymal-like morphology and a single cell pattern of growth. In low-adherent conditions, thyroid cancer cells established cell-to-cell contacts and formed multi-cellular spheroids. In FTC and ATC cells, formation of intercellular contacts was delayed compared to PTC-derived cells, but all thyroid cancer cell lines formed spheroids by 24 h after plating (Fig. 1A).

There was no evidence of cell death in thyroid cancer cells forming spheroids as determined by propidium iodine staining (data not shown). The viability of thyroid cancer cells in spheroids was assessed by detection of mitochondrial membrane potential using JC-1 staining. In all cell lines growing in low-adherent conditions, we observed formation of J

aggregates, indicating that these cells were viable (Fig. 1B). Thyroid cancer cells forming spheroids were able to adhere and restored a single cell pattern of growth after re-plating on the regular adherent plates (Fig. 1C).

Expression of adhesion molecules in thyroid cancer cell forming spheroids

Establishment of cell-to-cell contacts and the morphological changes in thyroid cancer cells that we observed during growth in low-adherent conditions suggested the potential role of cell adhesion molecules in the formation of spheroids. Analysis of previously published micro-array data (Vasko *et al.* 2007) revealed a differential expression of cell adhesion molecules (*N*-cadherin, integrin α6, integrin β4, Connexin31, and Connexin43) in human thyroid cancers compared to corresponding normal thyroid tissue. Therefore, we compared expression of these molecules in thyroid cancer cells forming spheroids and in corresponding adherent cells. The level of *N*-cadherin, integrin α6, integrin β4, and Connexin31 was not significantly different between adherent and non-adherent thyroid cancer cells (Supplementary Figure 1, see section on supplementary data given at the end of this article).

However, Connexin43 was differently expressed in cancer cell lines growing in adherent versus non-adherent conditions (Fig. 2A). Quantification of Connexin43 expression was performed after normalization to β-actin and results are summarized in Fig. 2B. Connexin43 expression was significantly increased in PTC- and ATC-derived thyroid cancer cell lines, but not in FTC-derived cancer cells. We also compared intracellular localization of Connexin43 in thyroid cancer cells growing on adherent plates and in low-adherent conditions. Immunostaining revealed cytoplasmic localization of Connexin43 in all examined thyroid cells growing on adherent plate, but predominantly membranous localization of Connexin43 in thyroid cancer cells growing in low-adherent conditions (Fig. 2C).

Activation of gap junctional intercellular transfer in thyroid cancer cell forming spheroids

Translocation of Connexin43 to the cell membrane in all cancer cells forming spheroids suggested that Connexin43-mediated gap junctional intercellular transfer (GJIT) could be induced in these cells. To determine the level of GJIT in thyroid cancer cells forming spheroids, we performed a fluorogenic dye transfer assay. Microscopy showed that calcein transfer from donor to recipient cells was higher in cancer cells forming spheroids compared with adherent cells (Fig. 3A). Quantification of calcein transfer was performed in cancer cells growing in adherent and low-adherent conditions and results are presented in Fig. 3B. The level of GJIT in PTC-derived cells forming spheroids was higher than that in other examined cell lines.

Together, these data showed that Connexin43 membranous re-localization with subsequent induction of GJIT is a common event in all examined thyroid cancer cells forming spheroids.

Growth of thyroid cancer cells in low-adherent condition

Since formation of cell-to-cell contacts is a known factor controlling cancer cell proliferation, we then examined the pattern of thyroid cancer cell growth in adherent and

low-adherent conditions. Growth of adherent TPC1, FTC236, FTC238 and SW1736 cells was higher when compared to the corresponding cells growing in the low-adherent condition during 24 h after plating. Growth of adherent FTC133 and BCPAP thyroid cancer cells was similar to the growth of those observed on non-adherent plates during the first 24 h after plating. The rate of growth, however, was decreased in all non-adherent cells incubated for 48, 72 and 96 h compared to adherent cells (Fig. 4A). Despite a decreased rate of growth, the viability of non-adherent cells, as determined by JC-1 staining, was not affected.

We also examined the pattern of thyroid cancer cell growth in serum-free medium. Serum deprivation was associated with progressive decrease in cell number and loss of viability in all examined cell lines cultured on adherent plates (Fig. 4B). In contrast, growth and viability of thyroid cancer cells cultured on low-adherent plates were not significantly affected by serum deprivation. Thyroid cancer cells growing in low-adherent condition were able to survive for up to 4 weeks without serum supplementation and restored growth after re-plating on adherent plate.

Flow cytometry showed that growth in low-adherent condition was associated with an increased proportion of cells in the G1 phase of the cell cycle and a decreased number of cells in G2/M phases. The proportion of cells in the sub-G1 phase was not different between adherent and non-adherent cells (data not shown). A common feature for all cancer cells forming spheroids was increased nuclear expression of p27 compared with corresponding adherent cells (Fig. 4C). The proportion of thyroid cancer cells showing nuclear expression of p27 in adherent and non-adherent condition was established by microscopic analysis of at least 250 cells in each of examined thyroid cancer cell lines and results are summarized in Fig. 4D.

Different patterns of thyroid cancer cell growth in adherent and low-adherent conditions were associated with different responses to a chemotherapeutical compound targeting proliferating cancer cells. In all examined thyroid cancer cells, treatment with docetaxel (10 μM for 24 h) was associated with changes in nuclear morphology. Treatment with docetaxel for 48 h induced cell death in adherent thyroid cancer cells but had limited effects on cancer cells cultured in low-adherent conditions (Supplementary Figure 2, see section on supplementary data given at the end of this article).

Together, these results showed that thyroid cancer cells growing in low-adherent conditions are characterized by a decreased proliferation rate and are more resistant to apoptotic stimuli compared with adherent cells.

Activation of anti-apoptotic signaling in thyroid cancer cell spheroids

The level of AKT activation in adherent thyroid cancer cells and in cell spheroids was examined by western blot and immunostaining. In FTC133, FTC236, FTC238, and TPC1 cancer cells growing in complete medium, the level of activated AKT was not significantly different between adherent and non-adherent cells (Fig. 5A). In BCPAP, KTC1, and SW1736 thyroid cancer cells, loss of attachment to extra-cellular matrix was associated with increased AKT activation. Serum deprivation was associated with a decrease in pAKT in

adherent cells. However, a high level of pAKT was detected in non-adherent thyroid cancer cells cultured in serum-free medium (Fig. 5A and 5B).

To confirm the role of PI3K/AKT signaling in resistance to anoikis, we examined the effect of LY294002 and its structural analog LY303511. Differential response to PI3K/AKT inhibitor was observed in thyroid cancer cells expressing a high level of PTEN (WRO, TPC1, BCPAP, and SW1736) and in PTEN-deficient cells (FTC133, FTC236, and FTC238). In PTEN-expressing thyroid cancer cell lines, treatment with LY294002 (10 μM for 24 h), but not with LY303511 (10 μM for 24 h), was associated with decreased activation of AKT (Fig. 5C). Inhibition of pAKT by LY294002 in non-adherent thyroid cancer cells was associated with induction of apoptosis in RET/PTC-positive cells (TPC1) as well as in BRAF mutant cell lines (BCPAP, KTC1, and SW1736).

In PTEN-deficient cells (FTC133, FTC236, and FTC238), treatment with LY294002 (10 μM for 24 h) resulted in minor inhibition of pAKT. However, extended treatment with LY294002 for 48 h or at increased concentration (20 μM) resulted in inhibition of pAKT and induction of apoptosis in these cell lines (data not shown). Treatment with LY303511 did not induce apoptosis in any examined cells growing on adherent or low-adherent plates.

Together, these results showed that activation of PI3K/AKT signaling plays a role in thyroid cancer cell resistance to anoikis.

Silencing of Connexin43 and thyroid cancer cell resistance to anoikis

Gap junctions serve as a conduit of inter-cellular transfer of messengers that can potentially activate AKT signaling; therefore, we hypothesized that there may be a link between activation of GJIT and resistance to anoikis in thyroid cancer cells. We first investigated whether inhibition of Connexin43 expression in thyroid cancer cell lines could affect their viability in low-adherent conditions. FTC133, TPC1, BCPAP, and SW1736 cells were transfected with Connexin43-specific siRNA or with scramble siRNA. The efficiency of transfection was evaluated with BLOCK-iT Fluorescent Oligo and ranged from 60 to 75%. The mRNA level of Connexin43 was inhibited by 25.6 ± 1.8-fold in FTC133, 10.2 ± 1.4-fold in TPC1, 17.2 ± 1.6-fold in BCPAP, and 21.3 ± 1.2-fold in SW1736 cells compared with corresponding cells transfected with scramble siRNA. The downregulation of Connexin43 was also confirmed by western blot analysis (Fig. 6A).

In adherent conditions, silencing of Connexin43 was not associated with inhibition of pAKT in any of the examined thyroid cancer cell lines. In low-adherent conditions, inhibition of Connexin43 had no effect on AKT activation in PTEN-deficient FTC133 cells. However, in TPC1, BCPAP, and SW1736 cells growing in low-adherent conditions, silencing of Connexin43 was associated with decrease in pAKT (Fig. 6B).

The viability of FTC133 cells in low-adherent condition was not significantly affected by Connexin43 silencing (Fig. 6C). The viability of TPC1, BCPAP, and SW1736 cells in low-adherent conditions was decreased after Connexin43 silencing.

Together, these data showed that Connexin43 has a variable contribution to AKT activation and resistance to anoikis in thyroid cancer cells lines with different oncogene mutations.

Resistance to anoikis was not significantly affected by the loss of Connexin43 in PTEN-deficient cells.

Pharmacological inhibition of gap junctional communication and thyroid cancer cell resistance to anoikis

We also examined the effects of a pharmacological disruptor of gap junctions (carbenoxolone) on thyroid cancer cells growing in adherent and low-adherent conditions. Carbenoxolone is reported to be effective as a gap junction uncoupler at concentrations ranging from as low as 3 μM to as high as 400 μM, in a cell-type-specific manner (Davidson *et al*. 1986, Bao *et al*. 2011). In adherent thyroid cancer cells, treatment with carbenoxolone (25 μM) did not affect cell viability in any of the cell lines (data not shown). In low-adherent conditions, carbenoxolone at 25 μM was associated with inhibition of GJIT in all cell lines, but most notably in PTC-derived thyroid cancer cells (Fig. 7A). Treatment of cell spheroids with increasing concentrations of carbenoxolone resulted in decreased cell viability in a dose-dependent manner (Fig. 7B). Carbenoxolone (25 μM) induced caspase cleavage in non-adherent WRO, TPC1, BCPAP, KTC1, and SW1736 cell lines (Fig. 7C). However, in PTEN-deficient cells (FTC133, FTC236, and FTC238), treatment with carbenoxolone from 25 to 50 μM was not associated with induction of apoptosis. However, with carbenoxolone at a concentration of 100 μM, cell death occurred in all examined cell lines growing on adherent and low-adherent plates.

As a known inhibitor of 11 β-hydroxysteroid dehydrogenase type 2, carbenoxolone increases the level of cortisol, which in turn leads to activation of glucocorticoid and mineralocorticoid receptors. To determine whether pro-apoptotic properties of carbenoxolone were related to inhibition of GJIT or to stimulation of corticoid receptors, we examined the effects of dexamethasone and aldosterone on thyroid cancer cells formed into spheroids. Treatment with dexamethasone or aldosterone (1–500 nm) had no effect on the viability of thyroid cancer cells growing in adherent and low-adherent conditions.

These findings demonstrated a cell-type-specific response to treatment with pharmacological disruptor of gap junction. Carbenoxolone had limited effect on resistance to anoikis in PTEN-deficient thyroid cancer cells.

AKT activation and Connexin43 expression in human thyroid cancer cells that invaded blood and lymphatic vessels

To determine whether these *in vitro* findings can have relevance *in vivo*, we examined serial tissue sections from 35 human papillary and ten FTCs. Thyroid cancer cells that had infiltrated blood and/or lymphatic vessels (Fig. 8A) were detected in 13/45 examined cases (ten PTCs and three FTCs). The intra-vascular thyroid cancer cells formed nests consisting of various numbers of cells. These cell aggregates were found in vessels located in the areas of extra-thyroidal tumor extension. In FTCs, floating cancer cell nests were covered by endothelial layer.

The thyroid origin of intra-vascular cell nests was confirmed by immunostaining with anti-thyroglobulin. Immunohistochemical evaluation of EMT markers (vimentin and *E*-cadherin) showed no differences between thyroid cancer cells located in the central area of tumors and

intra-vascular cells (data not shown). Consistent with previous studies, the intensity of pAKT staining was increased in the invasive front of tumors compared with cells located in the central part of tumors. Prominent activation of AKT was observed in intra-vascular thyroid cancer cells in both PTC and FTC (Fig. 8B). The level of Connexin43 expression was low or undetectable in all examined primary thyroid cancers. The level of Connexin43 expression was not significantly different between FTC cells located in central area of tumor and in intra-vascular cancer cells. In 6/10 PTCs with evidence of vascular invasion, intra-vascular cancer cells demonstrated increased Connexin43 immunoreactivity compared with cancer cells located in the central part of tumor (Fig. 8B).

Discussion

This study investigated the molecular mechanisms implicated in thyroid cancer cell resistance to anoikis and provides several novel findings. First, we showed that loss of extra-cellular matrix attachment is associated with the establishment of inter-cellular contacts and activation of GJIT between floating thyroid cancer cells. Secondly, we demonstrated that thyroid cancer cells forming spheroids are characterized by decreased proliferation with concomitant activation of anti-apoptotic AKT signaling. Thirdly, we provided evidence that resistance to anoikis is dependent on activation of GJIT in a cell-type-specific manner. Finally, we showed that human thyroid cancer cells located in blood or lymphatic vessels recapitulate the morphological features of spheroids (form interconnected cell aggregates) and have prominent AKT activation.

As a model, we employed a suspension culture on poly-HEMA-coated plates, conditions that inhibit cell–matrix interaction. In these conditions, thyroid cancer cells established cell-to-cell contacts and subsequently formed spheroid-like structures. Our findings are consistent with previously reported data. Formation of cancer cell aggregates has been reported in hepatoma, breast, prostate, and lung cancer cell lines growing in suspension (Berezovskaya *et al.* 2005, Liu *et al.* 2008, Zhang *et al.* 2008, Kochetkova *et al.* 2009). It has also been reported that formation of multi-cellular aggregates in non-adherent conditions is associated with over-expression of adhesion molecules (Zhang *et al.* 2008).

Analysis of adhesion molecules in thyroid cancer cells forming spheroids revealed the over-expression of the gap junction molecule Connexin43 only in PTC-and ATC-derived thyroid cancer cells. However, membranous translocation of Connexin43 was detected in all examined thyroid cancer cells growing in low-adherent conditions. Functional studies using a fluorogenic dye revealed activation of GJIT in all examined thyroid cancer cells forming spheroids.

These data suggested that Connexin43 membranous translocation with subsequent activation of GJIT is a common event in all thyroid cancer cells forming spheroids. This observation is in agreement with recently published findings demonstrating the importance of membranous Connexin43 localization for GJIT (Bodenstine *et al.* 2010).

Establishment of gap junctions affects a number of physiological functions such as cell growth, proliferation, and differentiation (Evans & Martin 2002). We showed that formation

of cell-to-cell contacts between thyroid cancer cells in low-adherent condition was associated with decreased proliferation. We also demonstrated that cancer cells in spheroids are more resistant to chemotherapeutic agents targeting proliferating cancer cells compared with adherent cells. Similar findings were previously reported in other cancer cell models (Sakuma *et al.* 2010).

Analysis of anti-apoptotic signaling revealed that AKT is constitutively activated in thyroid cancer cells forming spheroids. Resistance to anoikis in *BRAF* mutant thyroid cancer cells was also associated with increased AKT activation. These findings are consistent with previously published data showing the role of pAKT in cancer cell resistance to anoikis (Khwaja *et al.* 1997) and corroborate results demonstrating induction of pAKT in resistant to anoikis *BRAF*-positive melanoma cell lines (Boisvert-Adamo & Aplin 2006).

Our data also suggest that mechanisms controlling AKT activation could be different in adherent and non-adherent cancer cells. Formation of gap junctions facilitates intercellular transfer of cellular messengers (glucose, Ca^{2+}, IP3, camp, and others) that have the ability to activate AKT signaling. We hypothesized that inhibition of GJIT will decrease pAKT and sensitize thyroid cancer cells to anoikis. Silencing of Connexin43 was associated with decreased GJIT in thyroid cancer cells forming spheroids, especially in PTC-derived cells. Loss of Connexin43 was associated with inhibition of AKT activation and induction of apoptosis in thyroid cancer cell lines expressing a high level of PTEN. However, silencing of Connexin43 in a PTEN-deficient thyroid cancer cell line (FTC133 cells) was not associated with inhibition of pAKT and induction of apoptosis. PTEN-dexcient cells were also more resistant to treatment with a pharmacological disruptor of gap junctions. Together, these data showed that mechanisms underlying resistance to anoikis are cell-type specific and may be reliant on the mutation status of the examined cells, which is consistent with previously reported findings (Vitolo *et al.* 2009).

To determine whether our *in vitro* findings are relevant in human thyroid cancer, we examined human thyroid cancer cells that invaded blood or lymphatic vessels. In widely invasive thyroid cancers, we observed interconnected thyroid cancer cell aggregates located in blood or lymphatic vessels. These findings are similar to recently published data examining intralymphatic floating lung cancer cells (Sakuma *et al.* 2010). In addition to morphological resemblance with thyroid cancer cells forming spheroids *in vitro*, intravascular human thyroid cancer cells demonstrated prominent AKT activation. Analysis of Connexin43 expression in human thyroid cancers corroborated our *in vitro* data and suggested that Connexin43-mediated activation of GJIT can play a specific role in PTCs.

PTCs account for more than 80% of all thyroid cancers and are characterized by frequent metastatic spread to the loco-regional lymph nodes. Our data suggests that gap junction disruptors could target anoikis-resistant PTC cells and may have metastasis-preventive properties. Carbenoxolone is a water-soluble, synthetic derivative of the licorice root extract, 18-α-glycyrrhetinic acid, which inhibits gap junction communication (Sagar & Larson 2006). Carbenoxolone is used for the treatment of esophageal ulceration and inflammation at therapeutic dose of 0.714 mg/kg. Pharmacokinetic studies in humans showed that after administration of carbenoxolone at a dose of 4.5 mg/kg, its concentration in blood is only

142 nm. During treatment with these doses of carbenoxolone, blood pressure was significantly increased in the examined patients. The *in vitro* concentration necessary to affect anoikis is significantly higher than clinical applications have used, suggesting that it may be difficult to achieve a dose of carbenoxolone that would be tolerated in humans. However, other drugs are also known to disrupt gap junctional intercellular communication, to include anti-malarial (quinine and mefloquine), anti-inflammatory (fenamates), and anti-epileptic (phenytoin) drugs. Additional studies are needed to determine the possible effectiveness of these compounds for induction of anoikis in cancer cells.

In summary, our *in vitro* and *in vivo* data show that formation of cell-to-cell contacts with subsequent activation of GJIT plays a role in AKT activation and thyroid cancer cell survival in low-adherent conditions. On the basis of these findings, we propose that gap junction-mediated communication may represent a potential molecular target for prevention of metastases.

Supplementary Material

Refer to Web version on PubMed Central for supplementary material.

Acknowledgements

We thank Ildy Katona, Chair, Department of Pediatrics, USUHS, for her support for this project. We would also like to thank Dr Karen Marie Wolcott, PhD, of the Biomedical Instrumentation Center, Uniformed Services University of the Health Sciences, Bethesda, Maryland, for her assistance with flow cytometry.

Funding

This study was funded through the generosity of the Department of Pediatrics, Uniformed Services University of the Health Sciences (USUHS).

References

Bao B , Jiang J , Yanase T , Nishi Y & Morgan JR 2011 Connexon-mediated cell adhesion drives microtissue self-assembly. FASEB Journal 25 255–264. (doi:10.1096/fj.10-155291)20876208

Berezovskaya O , Schimmer AD , Glinskii AB , Pinilla C , Hoffman RM , Reed JC & Glinsky GV 2005 Increased expression of apoptosis inhibitor protein XIAP contributes to anoikis resistance of circulating human prostate cancer metastasis precursor cells. Cancer Res 65 2378–2386. (doi:10.1158/0008-5472.CAN-04-2649)15781653

Bodenstine TM , Vaidya KS , Ismail A , Beck BH , Cook LM , Diers AR , Landar A & Welch DR 2010 Homotypic gap junctional communication associated with metastasis suppression increases with PKA activity and is unaffected by PI3K inhibition. Cancer Research 70 10002–10011. (doi:10.1158/0008-5472.CAN-10-2606)21098703

Boisvert-Adamo K & Aplin AE 2006 B-RAF and PI-3 kinase signaling protect melanoma cells from anoikis. Oncogene 25 4848–4856. (doi:10.1038/sj.onc.1209493)16547495

Chappell WH , Green TD , Spengeman JD , McCubrey JA , Akula SM & Bertrand FE 2005 Increased protein expression of the PTEN tumor suppressor in the presence of constitutively active Notch-1. Cell Cycle 4 1389–1395. (doi:10.4161/cc.4.10.2028)16096376

Davidson JS , Baumgarten IM & Harley EH 1986 Reversible inhibition of intercellular junctional communication by glycyrrhetinic acid. Biochemical and Biophysical Research Communications 134 29–36. (doi:10.1016/0006-291X(86)90522-X)3947327

Evans WH & Martin PE 2002 Gap junctions: structure and function (review). Molecular Membrane Biology 19 121–136. (doi:10.1080/09687680210139839)12126230

Goldberg GS , Bechberger JF & Naus CC 1995 A pre-loading method of evaluating gap junctional communication by fluorescent dye transfer. Biotechniques 18 490–497.7779401

Hou P , Liu D , Shan Y , Hu S , Studeman K , Condouris S , Wang Y , Trink A , El-Naggar AK , Tallini G et al. 2007 Genetic alterations and their relationship in the phosphatidylinositol 3-kinase/Akt pathway in thyroid cancer. Clinical Cancer Research 13 1161–1170. (doi: 10.1158/1078-0432.CCR-06-1125)17317825

Khwaja A , Rodriguez-Viciana P , Wennstrom S , Warne PH & Downward J 1997 Matrix adhesion and Ras transformation both activate a phosphoinositide 3-OH kinase and protein kinase B/Akt cellular survival pathway. EMBO Journal 16 2783–2793. (doi:10.1093/emboj/16.10.2783)9184223

Kochetkova M , Kumar S & McColl SR 2009 Chemokine receptors CXCR4 and CCR7 promote metastasis by preventing anoikis in cancer cells. Cell Death and Differentiation 16 664–673. (doi: 10.1038/cdd.2008.190)19136936

Liotta LA & Kohn E 2004 Anoikis: cancer and the homeless cell. Nature 430 973–974. (doi: 10.1038/430973a)15329701

Liu G , Meng X , Jin Y , Bai J , Zhao Y , Cui X , Chen F & Fu S 2008 Inhibitory role of focal adhesion kinase on anoikis in the lung cancer cell A549. Cell Biology International 32 663–670. (doi: 10.1016/j.cellbi.2008.01.292)18343694

Sagar GD & Larson DM 2006 Carbenoxolone inhibits junctional transfer and upregulates Connexin43 expression by a protein kinase A-dependent pathway. Journal of Cellular Biochemistry 98 1543–1551. (doi:10.1002/jcb.20870)16552723

Sakuma Y , Takeuchi T , Nakamura Y , Yoshihara M , Matsukuma S , Nakayama H , Ohgane N , Yokose T , Kameda Y , Tsuchiya E et al. 2010 Lung adenocarcinoma cells floating in lymphatic vessels resist anoikis by expressing phosphorylated Src. Journal of Pathology 220 574–585. (doi: 10.1002/path.2676)20146241

Schweppe RE , Klopper JP , Korch C , Pugazhenthi U , Benezra M , Knauf JA , Fagin JA , Marlow LA , Copland JA , Smallridge RC et al. 2008 Deoxyribonucleic acid profiling analysis of 40 human thyroid cancer cell lines reveals cross-contamination resulting in cell line redundancy and misidentification. Journal of Clinical Endocrinology and Metabolism 93 4331–4341. (doi: 10.1210/jc.2008-1102)18713817

Thiery JP 2002 Epithelial–mesenchymal transitions in tumour progression. Nature Reviews. Cancer 2 442–454. (doi:10.1038/nrc822)12189386

Vasko V , Saji M , Hardy E , Kruhlak M , Larin A , Savchenko V , Miyakawa M , Isozaki O , Murakami H , Tsushima T et al. 2004 Akt activation and localisation correlate with tumour invasion and oncogene expression in thyroid cancer. Journal of Medical Genetics 41 161–170. (doi:10.1136/jmg.2003.015339)14985374

Vasko V , Espinosa AV , Scouten W , He H , Auer H , Liyanarachchi S , Larin A , Savchenko V , Francis GL , de la Chapelle A et al. 2007 Gene expression and functional evidence of epithelial-to-mesenchymal transition in papillary thyroid carcinoma invasion. PNAS 104 2803–2808. (doi: 10.1073/pnas.0610733104)17296934

Vitolo MI , Weiss MB , Szmacinski M , Tahir K , Waldman T , Park BH , Martin SS , Weber DJ & Bachman KE 2009 Deletion of PTEN promotes tumorigenic signaling, resistance to anoikis, and altered response to chemotherapeutic agents in human mammary epithelial cells. Cancer Research 69 8275–8283. (doi:10.1158/0008-5472.CAN-09-1067)19843859

Wang LH 2004 Molecular signaling regulating anchorage-independent growth of cancer cells. Mount Sinai Journal of Medicine 71 361–367.15592654

Weng LP , Gimm O , Kum JB , Smith WM , Zhou XP , Wynford-Thomas D , Leone G & Eng C 2001 Transient ectopic expression of PTEN in thyroid cancer cell lines induces cell cycle arrest and cell type-dependent cell death. Human Molecular Genetics 10 251–258. (doi:10.1093/hmg/10.3.251)11159944

Zhang Z , Cao L , Li J , Liang X , Liu Y , Liu H , Du J , Qu Z , Cui M , Liu S et al. 2008 Acquisition of anoikis resistance reveals a synoikis-like survival style in BEL7402 hepatoma cells. Cancer Letters 267 106–115. (doi:10.1016/j.canlet.2008.03.010)18433990

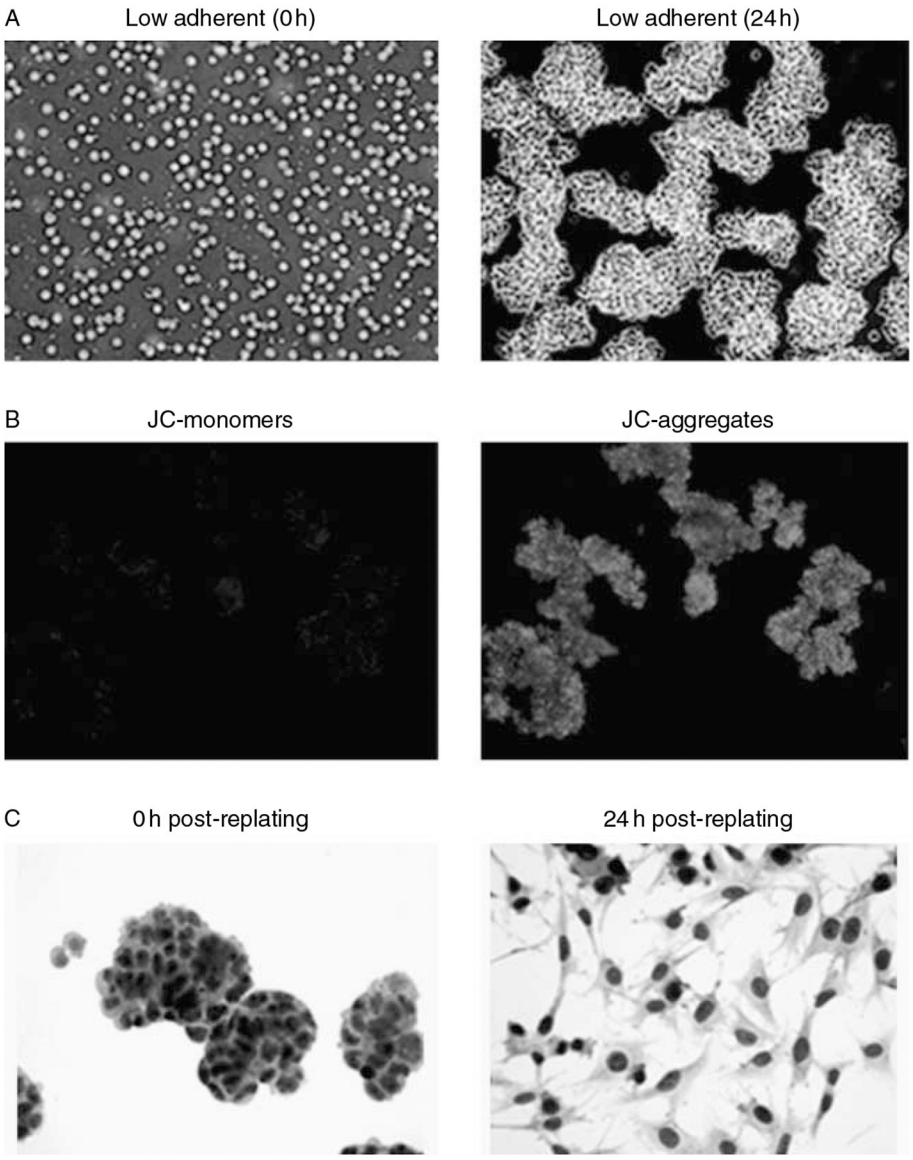

Figure 1.

Thyroid cancer cell morphology in low-adherent conditions. TPC1 cells demonstrate common phenomena to all cell lines. (A) Individual cells at initial plating in low-adherent conditions. At 24 h, each cell type was formed into multi-cellular, trabecula-like structures. (B) In low-adherent conditions, very low amount of fluorescence at 535 nm was seen, indicating a paucity of JC-1 monomers. Conversely, intense fluorescence at 570 nm was seen in JC-1 aggregates. (C) Cells in spheroids re-established a mesenchymal morphology by 24 h on adherent culture plates.

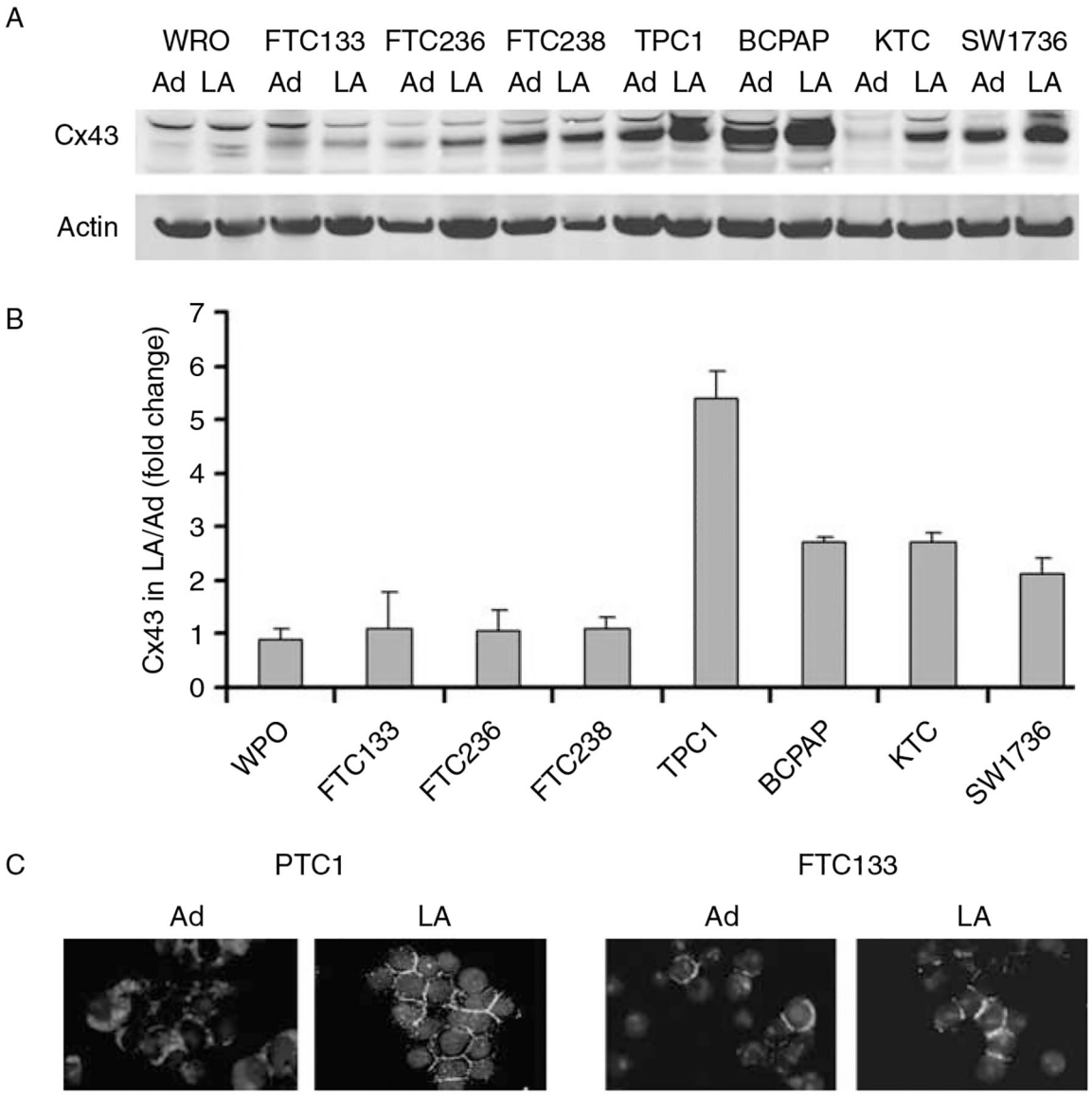

Figure 2.

Gap junction formation and inter-cellular communication. (A) Connexin43 (C×43) protein level in cancer cells grown in adherent and low-adherent conditions. (B) Graphical representation demonstrating induction of C×43 in low-adherent versus adherent conditions. (C) Increased membranous immunoreactivity of C×43 in non-adherent cell spheroids. Ad, adherent conditions; LA, low-adherent conditions.

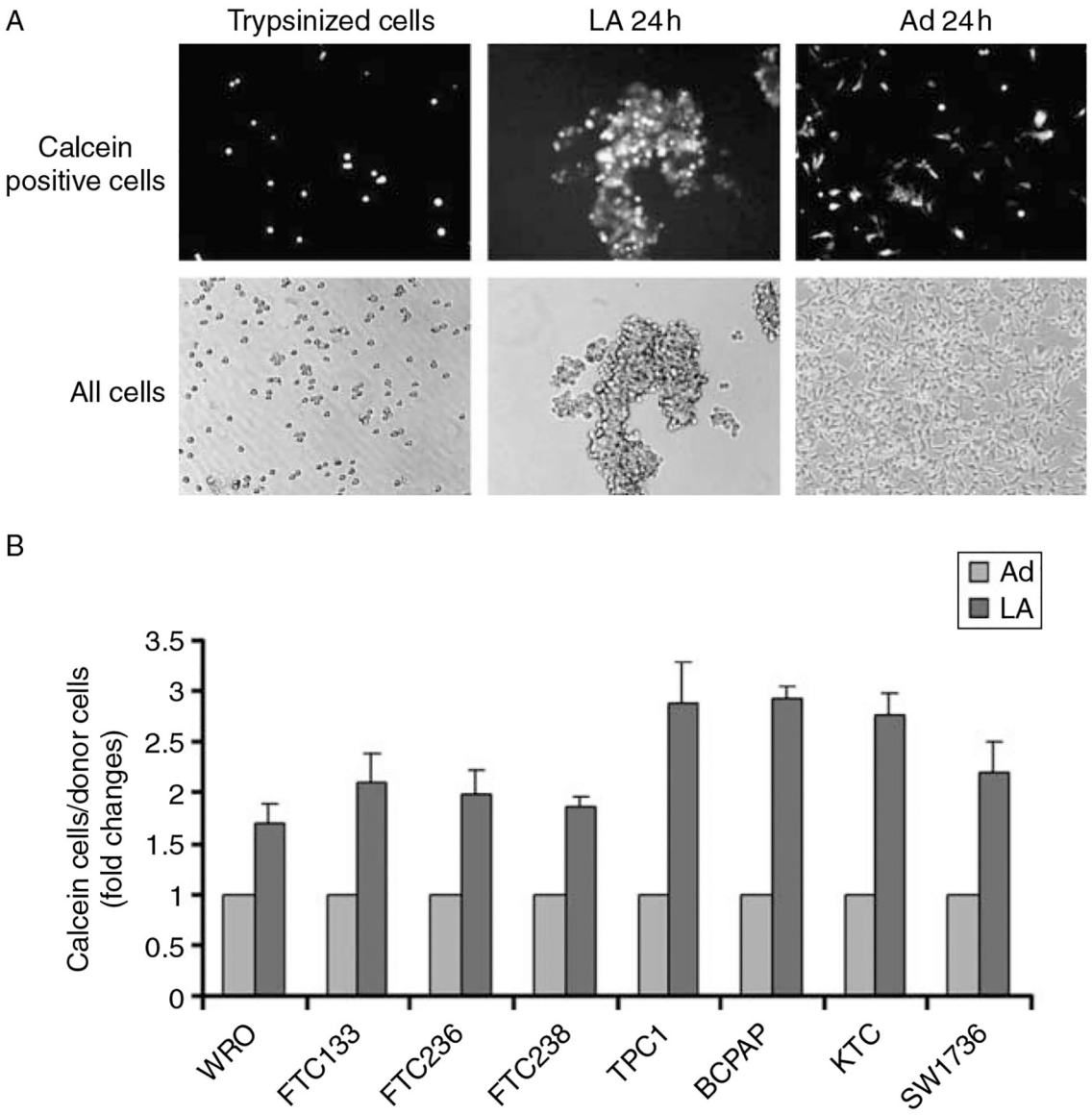

Figure 3.

(A) Increased calcein transfer in thyroid cancer cells forming spheroids versus adherent cells. (B) Calcein transfer occurs in all cell lines in spheroids, with more transfer occurring in PTC-derived cells. Ad, adherent conditions; LA, low-adherent conditions.

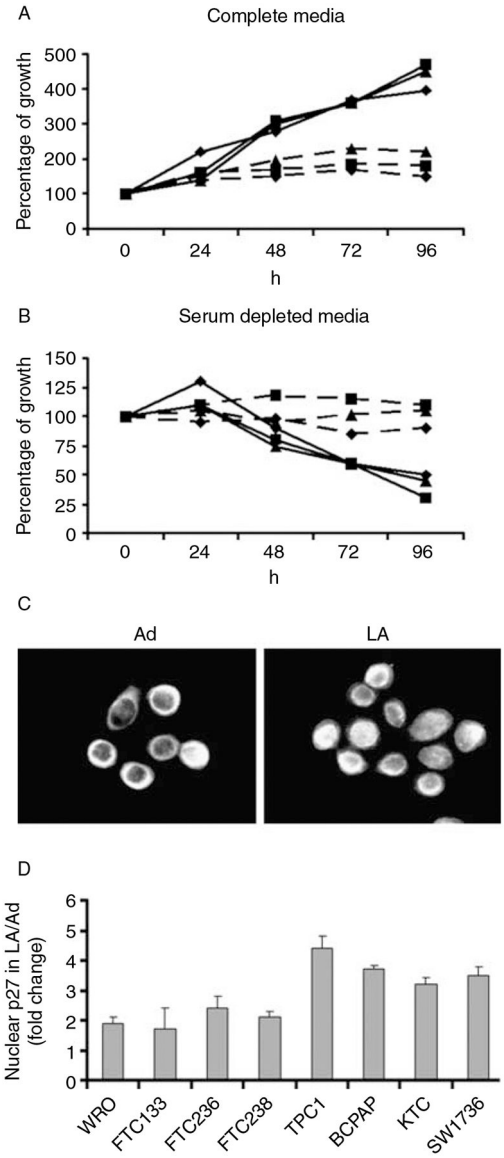

Figure 4.

Thyroid cancer cell growth in low-adherent conditions. For (A and B), the solid lines indicate growth curve of adherent cells and the dashed lines are representative of low-adherent conditions. Filled square, FTC133; filled diamond, TPC1; filled triangle, BCPAP. Cell growth and viability were examined by using Vi-CELL Cell Viability Analyzer. (A) Growth in complete media. (B) Growth in serum-free media. (C) Immunostaining indicating predominantly nuclear p27 in low-adherent conditions. (D) Growth in low-adherent condition is associated with increased number of cells with nuclear p27 expression. Ad, adherent conditions; LA, low-adherent conditions.

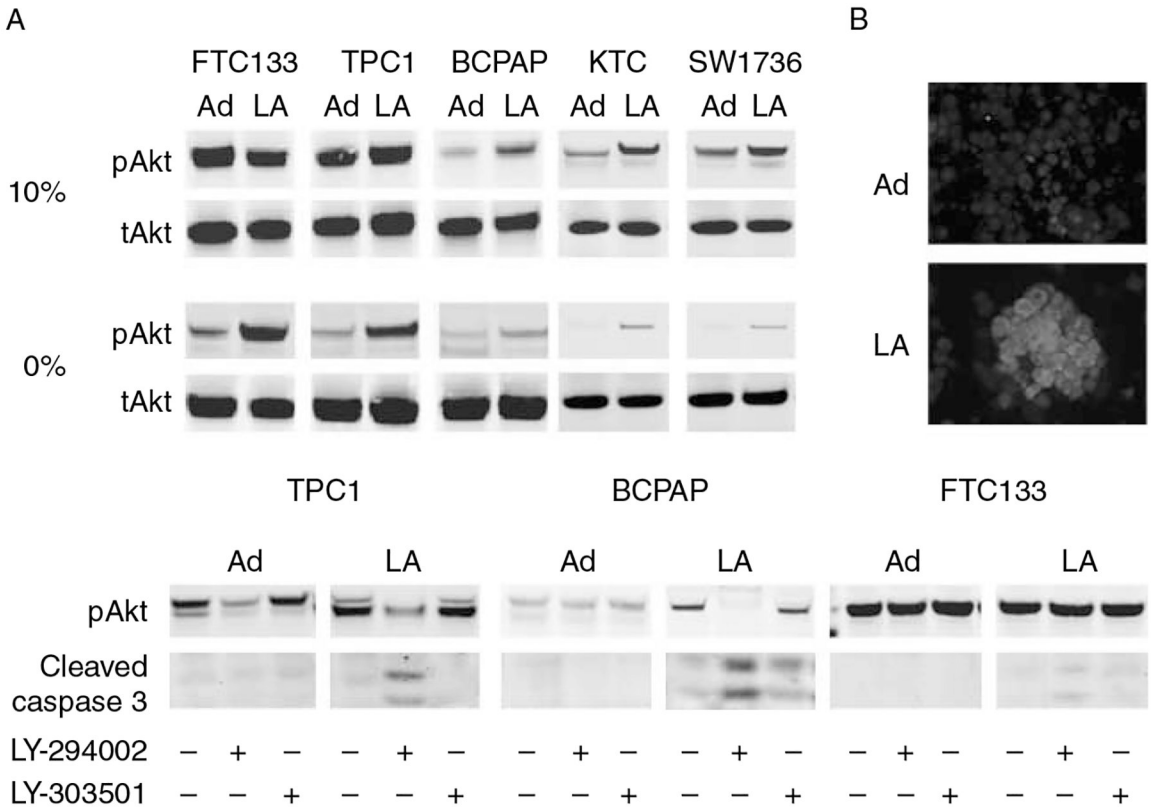

Figure 5.

AKT activation in thyroid cancer cells growing in adherent (A) and low-adherent (LA) conditions. (A) Cells were grown in complete (10%) or in serum-deprived (0%) medium and AKT activation was detected by western blot. (B) pAKT immunostaining in TPC1 cells culturing in serum-free media. (C) AKT activation in thyroid cancer cells after exposure to LY-294002 (10 μM) and LY-303501 (10 μM) in both adherent and low-adherent conditions. In non-adherent TPC1 and BCPAP cells, inhibition of pAKT was associated with induction of caspase cleavage. PTEN-deficient FTC cells showed increased resistance to treatment with LY-294002. Ad, adherent conditions; LA, low-adherent conditions.

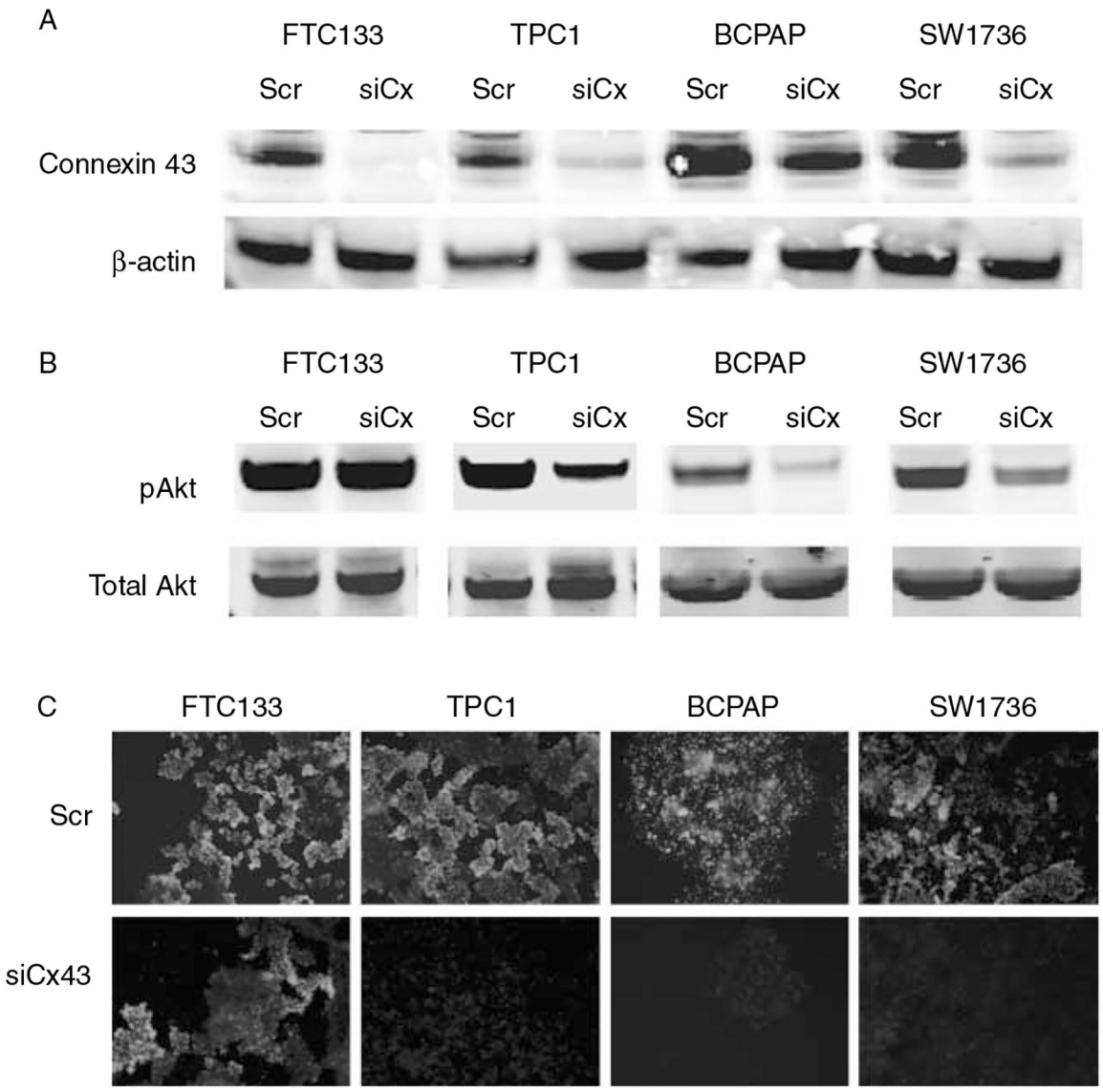

Figure 6.

The effect of Connexin43 silencing on thyroid cancer cells forming spheroids in low-adherent conditions. Scr, scramble. siCx, siRNA of C×43. (A) Gain of C×43 in low-adherent conditions was prevented by siRNA to C×43. (B) Loss of C×43 in non-adherent cells correlated with decreased AKT activation in TPC1, BCPAP, and SW1736 cells. (C) In low-adherent conditions, C×43 silencing was associated with decreased viability in TPC1, BCPAP, and SW1736 cells (paucity of JC aggregates), but had limited effect on the viability of FTC133 cells.

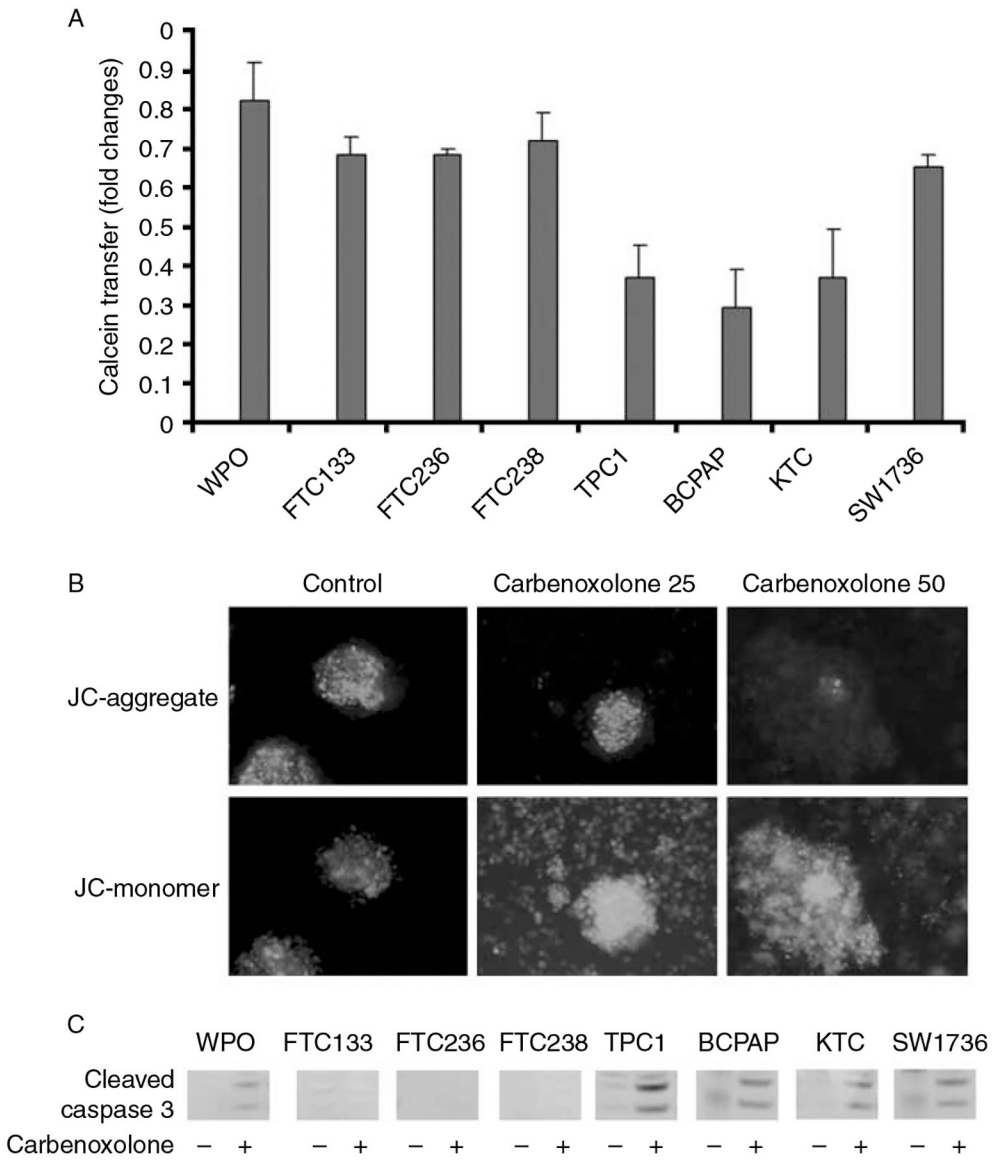

Figure 7.

The effect of a pharmacological inhibitor of gap junctional transfer on thyroid cancer cells. (A) Carbenoxolone treatment decreased calcein transfer in all cell lines, most notable in PTC-derived cells (60–70% decrease). (B) Carbenoxolone treatment sensitized non-adherent TPC1 cells to anoikis in a dose-dependent manner as evidenced by the progressive loss of JC aggregates and accumulation of JC monomers. (C) Non-adherent cells with or without carbenoxolone (25 μM). Caspase cleavage induced in WRO, TPC1, BCPAP, KTC1, and SW1736 cells.

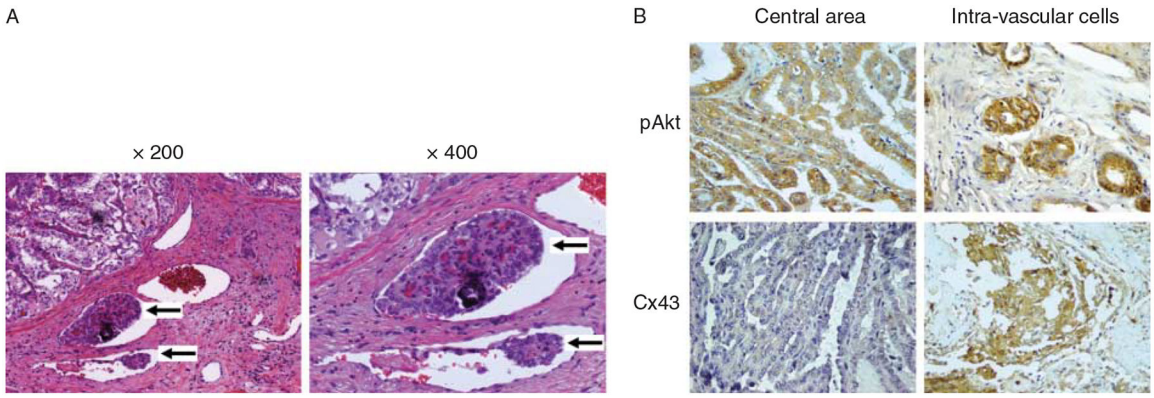

Figure 8.

Human thyroid cancer tissue samples. (A) H&E staining demonstrating intra-vascular thyroid cell aggregate (arrows). (B) Immunostaining with anti-pAKT and anti-C×43 antibodies in human thyroid cancer samples.